A hybrid approach to underwater docking of AUVs with cross-current

Albert Sans-Muntadas, Kristin Y. Pettersen, Edmund Brekke and Vegard F. Henriksen
Norwegian University of Science and Technology (NTNU)
Centre for Autonomous Marine Operations and Structures (AMOS)
Otto Nielsens veg 10, NO-7491 Trondheim, Norway
Email: {albert.sans, kristin.y.pettersen, edmund.brekke}@itk.ntnu.no, vegardfh@stud.ntnu.no

***Abstract*—This paper proposes a docking maneuver for an underactuated autonomous underwater vehicle (AUV) to dock into a funnel shaped docking station. The novelty of the proposed approach is enabling an underactuated AUV that is unable to control its sway motion, to dock with no crab angle, in the presence of cross-currents. Docking without a crab angle can be beneficial in cases where the geometry of the docking station entrance does not allow entering with crab angles.**

In order to successfully dock under such restrictions, a path planner and two guidance laws are proposed. By properly switching between the two guidance laws, it is possible for the vehicle to slide cross-current into the docking station.

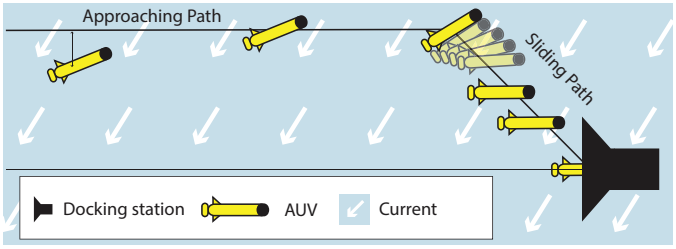

Fig. 1. Sketch of the maneuver progression

I. Introduction

Underwater vehicles routinely perform tasks such as bathymetric mapping, pipeline inspection, scientific data collection, geological surveys, under ice intervention or homeland security. While AUV technology has been proven to be mature, a common requirement which reduces the effectiveness and feasibility of AUV operations is the need of a surface support vessel. In missions lasting from hours, up to days or weeks, the needed surface vessel and infrastructure significantly contribute to increasing the cost, and also making the operational outcome more dependent on sea conditions.

Being able to autonomously launch and recover AUVs will make AUV technology more cost effective, safer and more robust. Also, it will enable having resident AUVs ready for subsea operations, which will further extend the capabilities of AUVs. A key technology for achieving this is autonomous docking of AUVs.

There have been various successful attempts in this autonomous docking endeavor, e.g. ([1], [2], [3], [4], [5], [6], [7], [8]). The most common solution is a funnel shaped entrance and a latching system that holds and connects the vehicle, together with a straight line trajectory that guides the vehicle inside the docking station [9], [10]. An underactuated AUV that cannot control its sway motion when following a straight path needs to move with a crab angle to compensate for the effects of currents acting transverse to the path. Unfortunately, in some cases this crab angle may make the docking task impossible due to the restrictions caused by the shape of the entrance, and some of the proposed docking controllers may therefore not be useful in such cases [11]. In order to solve this problem [11] suggests, inspired by the sideslip landing maneuver of planes performed with cross-winds, to align the heading instants before reaching the entrance of the docking station. In [12] it is proposed to follow a side lane parallel to the docking centerline, and when close to the docking station, shift into an aligned heading with the docking station.

The contribution of this paper consists of a path planner that takes into account the currents and leads the vehicle to the center of the docking station. Our proposed guidance, combined with an integral line of sight guidance (ILOS), allows the vehicle to have its heading aligned to the docking station centerline when reaching the entrance of the docking station trough the proposed path.

The paper is organized as follows: In Section II the proposed docking maneuver is described. In Section III a kinematic model of the AUV under the presence of currents is given. Section IV, defines formally the path and the control objectives for the maneuver. Section V formalizes the guidance laws that will allow the vehicle to follow the path. Section VI explains the proposed hybrid controller and proofs its stability. Section VII shows the simulation results and Section VIII concludes the paper.

II. Maneuver Description

The proposed maneuver consists of following a path divided in two parts: The *approaching path* and the *sliding path*. During the *approaching path*, the AUV follows a straight line parallel to the centerline of the docking station. Due to the presence of cross-current, the component of the current perpendicular to the path, the vehicle needs to keep a certain crab angle in order to stay on the path [13]. Once the vehicle gets closer to the docking station, it changes to the *sliding path* that leads to the entrance of the docking station. The *sliding path* is designed such that the crab angle, necessary to

follow the path under the presence of cross-current, makes the heading align with the docking entrance centerline.

The end goal for this maneuver is to reach the entrance of the docking station with a docking velocity, $u = U_{doc}$, and with a heading parallel to the entrance of the docking station, $\psi_d = \psi_{doc} = 0$ (See Fig.1). To achieve these objectives, a hybrid guidance law is defined in Section V using a hybrid control framework [14].

III. The Model

The motion of the AUV in the horizontal plane is described by the position and orientation of the vessel w.r.t. to the docking station. The state vector is given by $[x, y, \psi]$. The ocean current, expressed also in the same frame, is denoted by V_x, V_y. The docking maneuver is designed for the type of underactuated AUVs that can control the surge and yaw motion, but cannot control the sway. The following assumptions are made to describe the AUV model:

Assumption 1. *The motion of the AUV can be described in 3 degrees of freedom: Surge, sway and yaw. But sway << surge and only affects the transient therefore is neglected.*

Assumption 2. *The AUV is underactuated in sway but not in surge and yaw, and the internal controllers are able to achieve the desired velocity U_{rd} and yaw ψ_d.*

Assumption 3. *The ocean current is assumed to be constant, irrotational and bounded, and the desired relative velocity U_{rd} is always bigger than the ocean current $\sqrt{V_x + V_y}$.*

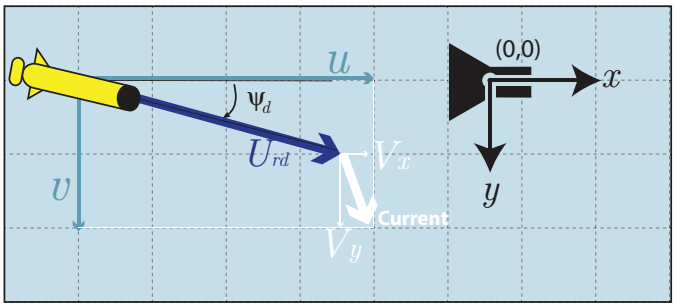

Fig. 2. Coordinate system

Shen the guidance laws are tuned to avoid sharp turns applying assumptions (1-3) become reasonable and makes the problem a pure kinematic problem. Then the system is described by the following model:

$$\dot{x} = U_{rd}\cos(\psi_d) + V_x \tag{1a}$$
$$\dot{y} = U_{rd}\sin(\psi_d) + V_y \tag{1b}$$

IV. Path Following Problem

The shape of the path is determined by the following parameters: the length l of the sliding path and the course of the *sliding path* χ_s which is the angle between docking velocity U_{doc} and an estimate of the current that is perpendicular to the docking centerline $\hat{V}_y$.

$$\tan(\chi_s) = \frac{\hat{V}_y}{U_{doc}} \tag{2}$$

The mathematical description for the *approaching path* and the *sliding path* can be written as:

$$\mathcal{P} := \left\{ x, y \in \mathbb{R}^2 \;\middle|\; \begin{array}{lll} y = -l\sin(\chi_s) & x < -l\cos(\chi_s) & \textit{Approaching path} \\ y = x\tan(\chi_s) & -l\cos(\chi_s) \le x \le 0 & \textit{Sliding path} \end{array} \right\} \tag{3}$$

where the course of the path $\chi_p = 0$ for the *Approaching path* and $\chi_p = \chi_s$ *Sliding path*.

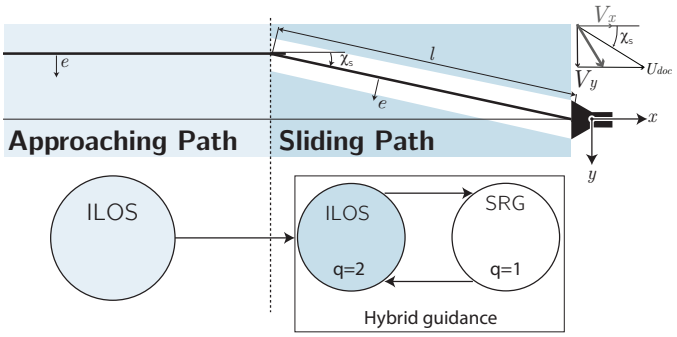

Fig. 3. Sketch of the path, the parameters that describe the path, and the guidances applied at each part of the path

A. Approaching path

The *approaching path* is parallel to the docking station centerline and at a certain offset on the "upcurrent" side of the centerline. The control objectives along this path can be described as follows:

$$\lim_{t\to\infty} e(t) = 0 \tag{4a}$$
$$\lim_{t\to\infty} \psi_d(t) = \psi_{ss} \tag{4b}$$
$$\lim_{t\to\infty} U_{rd}(t) = U_{doc} - \hat{V}_x \tag{4c}$$

where ψ_{ss} is the crab angle necessary to compensate for the cross-current and e is the cross-track error to the path. For the approaching path the error is described as:

$$e = -l\sin(\chi_s) - y \tag{5}$$

B. Sliding path

The *sliding path* is a straight line that leads to the center of the docking station with coordinates $[x, y] = [0, 0]$ and it has the same direction as a vehicle aligned with the docking station that moves at a surge speed U_{doc} with the presence of a current V_y.

The control objectives on the *sliding path* are:

$$\lim_{t\to\infty} e(t) = 0 \tag{6a}$$
$$\lim_{t\to\infty} \psi_d(t) = \psi_{ss} - \chi_s = 0 \tag{6b}$$
$$\lim_{t\to\infty} U_{rd}(t) = U_{doc} - \hat{V}_x \tag{6c}$$

The cross-track error to the *sliding path* is described as:

$$e = -x\sin(\chi_s) + y\cos(\chi_s) \tag{7}$$

These objectives will be achieved by two guidance laws described in Section V that are combined together with a hybrid controller described in Section VI.

V. Control and Guidance Laws

This section presents the guidance laws used to achieve the docking maneuver described in Section II under the objectives described in Section IV. During the approaching path, the vehicle is guided by an Integral Line of Sight (ILOS) [13] guidance law (see 3). Then, when the vehicle reaches the *sliding path*, two guidance laws, an ILOS and a Speed Regulated Guidance (SRG), are combined with a hybrid framework in order to achieve the objectives 6a-6c.

The desired yaw ψ_d and velocity U_{rd} prescribed by the guidance laws are achieved by two internal controllers that adjust the rudder and the thrust in order to match the desired ones.

Assumption 4. *It is assumed that the vessel has reliable knowledge of the vehicle surge and sway velocity, u and v, and that it is able to estimate the current $\hat{V}_x$ and $\hat{V}_y$. The vehicle is furthermore able to maintain a constant relative surge speed U_r.*

Remark 1. *Reliable knowledge of the vehicle velocities u and v can for instance be achieved using an underwater acoustic positioning system like a USBL system, or by using a DVL with bottom lock. Ocean current estimates can be achieved through an observer, for instance [15] or through lookup tables. Based on these measurements and estimates, or using a DVL without bottom lock, the relative surge speed is measured/calculated, and a speed controller like for instance the feedback linearizing speed controller in [13] will maintain the desired relative surge speed U_{rd} with exponential convergence.*

A. ILOS Guidance

The ILOS guidance law is used for following a straight line path in the presence of unknown currents. By using integral action e_{int} the ILOS guidance law is able to estimate a side-slip angle that will compensate the effect of cross-currents, and make the vehicle to converge to the path. The following ILOS guidance law is a particular version of the LOS guidance control law presented in [13], for which uniform global asymptotic stability (UGAS) is shown, ensuring that control objectives (4a-4c, 6a-6c) are achieved.

$$\psi_d = \chi_p - \operatorname{atan}\left(\frac{e + \sigma e_{int}}{\Delta}\right) \tag{8}$$

In order to avoid windup effects on the integral an anti-windup function is used:

$$\dot{e}_{int} = \frac{\Delta e}{(e + \sigma e_{int})^2 + \Delta^2} \tag{9}$$

The desired relative velocity U_{rd} is designed to make the vehicle approximately match U_{doc} in the final event of docking when the vehicle is aligned with the docking station.

$$U_{rd} = U_{doc} - \hat{V}_x \tag{10}$$

From the results in [13], we see that the ILOS guidance law (8) makes the vehicle follow the path. When the vehicle is following the *sliding path* with the desired speed (6c), the crab angle needed to compensate for the current makes the vehicle align with the docking entrance ($\psi = 0$). Note that some misalignment may occur if the vehicle has imprecise estimation of the current $[V_x, V_y]$, or a poor knowledge of the vehicle's relative velocity U_r. For this reason, we propose the combination of the ILOS and the SRG.

For sake of simplicity in both the programming and the following mathematical proofs, the states are unified into $z = [e, \psi_d]^\top$ instead of using e_{int} as in [13]. The desired yaw becomes then, a state and the dynamics of ψ_d are obtained by substituting (8) and (9) into the derivative of (8).

$$\dot{\psi}_d = -\cos^2(\psi_d - \chi_s)\frac{\Delta\dot{e} - \sigma e\cos^2(\psi_d - \chi_s)}{\Delta^2} \tag{11}$$

The Lyapunov function used to show UGAS for the ILOS in [13] can be reformulated with the states e, ψ_d as:

$$V(z) = \frac{1}{2}\left(\tan(\psi_d - \chi_s) + \tan(\chi_s) + \frac{e}{\Delta}\right)^2 + \frac{1}{2}\left(\tan(\psi_d - \chi_s) + \tan(\chi_s)\right)^2 \tag{12}$$

B. Speed Regulated Guidance (SRG)

In order to prevent misalignments caused by imprecise knowledge of the current or the vehicle's relative speed that might occur under the ILOS, a new guidance law, the SRG is presented in this paper.

The SRG is only used along the *sliding path* and is switched on when the vehicle is very close (see details in Section VI) to the *sliding path*. The SRG enforces the vehicle to be parallel to the docking station and since the distance to the path can no longer be adjusted by changing the yaw, the vehicle instead adjusts its surge within a speed limitation U_m to maintain itself on the *sliding path*.

$$\psi_d = 0 \tag{13}$$

$$U_{rd} = \underbrace{\frac{v}{\gamma}}_{\approx U_{doc}} - \hat{V}_x - U_m\tfrac{2}{\pi}\operatorname{sign}(\chi_s)\operatorname{atan}(k_u e) \tag{14}$$

Note that SRG can only be used under the presence of currents because the vehicle is forced to lock the yaw parallel to the docking station, and the current is thus necessary to move forward along the path. Using SRG provides the AUV with stronger accuracy on the heading. It also allows to align the vehicle with the docking station centerline under uncertain currents.

VI. Hybrid Guidance

Along the *sliding path* a combination of the previously described guidances (ILOS and SRG) under a hybrid framework is used in order to benefit from both and achieve the control objectives (6a-6c) with more robustness.

The hybrid system switches between ILOS and SRG, indicated by a logic state $q \in Q$ where $Q = \{1, 2\}$. The ILOS ($q = 2$) described in Section V-A makes the AUV satisfy the control objectives (4a-4c) under the assumptions 1-4. The SRG ($q = 1$) ensures that control objectives (6a-6c) are satisfied.

In the terminology of hybrid systems C sets are often referred as flows sets and represent the sets where continuous dynamics are allowed. The D sets also called jumps sets, are the sets where discontinuous dynamics are allowed. In this paper a switch between guidance law only happens when the vehicle reaches a region D.

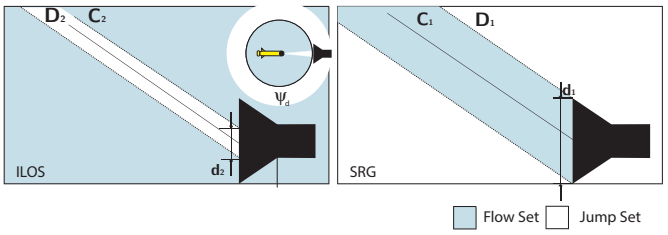

Fig. 4. Representation of the sets C_1, C_2, D_1, D_2 for the hybrid guidance that dictates the switches among ILOS and SRG.

The hybrid guidance allows to switch between ILOS and SRG according to the position of the vehicle within the sets C_1, C_2, D_1, D_2 (see Figure 4). The vehicle normally begins by using the ILOS guidance (q=2, left plot). When the vehicle enters the *sliding path*, the ILOS law makes it converge to the path. As it enters D_2 the guidance switches to SRG ($q = 1$, right plot) until docking. If a disturbance caused the vehicle to leave region C_1, it would switch back to the ILOS ($q = 2$) guidance. This would allow it to use again the heading to adjust the course and reach the *sliding path* faster, until it switches again to SRG.

In Figure 4 regions C_1 and C_2 (shaded in blue) represent the regions where the vehicle is allowed to flow. In white D_1 and D_2 are the regions where the vehicle will change guidance law. C_1 is a region for which the cross-track error e is smaller than the diameter of the docking station entrance d_1 projected in the direction of the *sliding path* ($|e| \leq d_1 \cos(\chi_s)$). It can also be interpreted as a safe-zone where a vehicle maintaining a course χ_s would finish inside the docking station. D_2 region allows to switch from ILOS to SRG, and is inside the safe-zone. Note that D_2 is smaller than C_1 to introduce a hysteresis that will avoid chattering between guidances due to disturbances caused by turbulence, vehicle dynamics or sensor error.

A. Definition of the hybrid system

The mathematical description of the sets C and D (illustrated in Figure 4) is:

$$\begin{aligned} C_1 &= \left\{ e \in \mathbb{R}^2 : |e| \leq d_1 \cos(\chi_s) \cap \{\psi_d = 0\} \right\} \\ D_1 &= \overline{\{\mathbb{R}^2\}/C_1} \\ C_2 &= \{e, \psi_d \in \mathbb{R}^2 : \{|e| \leq d_2 \cos(\chi_s)\} \cap \{|\psi_d| \leq \psi_{max}\} \\ D_2 &= \overline{\{\mathbb{R}^2\}/C_2} \end{aligned} \tag{15}$$

The closed-loop system resulting from controlling the nonlinear system (1a-1b) with the hybrid controller $F_q(e, \psi_d)$ is given by $F_1(z)$ when using ILOS:

$$F_1(z) = \begin{bmatrix} \dot{e} \\ \dot{\psi}_d \end{bmatrix} = \begin{bmatrix} U_{rd} \sin(\psi_d - \chi_s) - V_x \sin(\chi_s) + V_y \cos(\chi_s) \\ -\cos^2(\psi_d - \chi_s) \frac{\Delta \dot{e} + \sigma e \cos^2(\psi_d - \chi_s)}{\Delta^2} \end{bmatrix} \tag{16}$$

and $F_2(z)$ when using SRG:

$$F_2(z) = \begin{bmatrix} \dot{e} \\ \dot{\psi}_d \end{bmatrix} = \begin{bmatrix} -\frac{\pi}{2} |\sin(\chi_d)| U_m \operatorname{atan}(k_u e) \\ 0 \end{bmatrix} \tag{17}$$

When the system switches guidance laws ψ_d experiences an instantaneous jump and becomes zero as described in (13).

$$g(z) = \begin{bmatrix} e^+ \\ \psi_d^+ \end{bmatrix} = \begin{bmatrix} e \\ 0 \end{bmatrix} \tag{18}$$

The index $(^+)$ denotes an instantaneous jump in the state.

The logic variable q and the states e,ψ_d are collected in a state vector η :

$$\eta = \begin{bmatrix} q \\ e \\ \psi_d \end{bmatrix} \in Q \times \mathbb{R}^2 \tag{19}$$

The hybrid system is written formally as $\mathcal{H} = \{C, F, D, G\}$:

$$\begin{aligned} C &= \bigcup_{q \in Q} \{\{q\} \times C_q\}, \quad F(z) = \begin{bmatrix} 0 \\ F_q(z) \end{bmatrix}, \\ D &= \bigcup_{q \in Q} \{\{q\} \times D_q\}, \quad G(z) = \begin{bmatrix} 3 - q \\ g(z) \end{bmatrix}. \end{aligned} \tag{20}$$

B. Stability proof of the Hybrid system

If the assumptions 1-4 hold, the set $\mathcal{A} := \{\eta : q = 1, e = 0, \psi_d = 0\}$ is uniformly (pre-) asymptotically stable for the hybrid system $\mathcal{H}$

Proof. First we consider the Lyapunov candidate V described in (12) which satisfies [14, (3.2a)] $\forall s \in \mathbb{R}_{\geq 0}$:

$$\begin{aligned} \alpha_1(s) &:= \min \left\{ \tfrac{1}{2} \left(\tan(s - \chi_s) + \tan(\chi_s) + \frac{s}{\Delta} \right)^2, \tfrac{1}{2} \left(\tan(s - \chi_s) + \tan(\chi_s) \right)^2 \right\} \\ \alpha_2(s) &:= \tfrac{1}{2} \left(\tan(s - \chi_s) + \tan(\chi_s) + \frac{s}{\Delta} \right)^2 + \tfrac{1}{2} \left(\tan(s - \chi_s) + \tan(\chi_s) \right)^2 \end{aligned} \tag{21}$$

There exists an open neighborhood $\mathcal{U}_1$ of the origin and a function $\rho_1 \in \mathcal{PD}$ such that:

$$\langle \nabla V(z), F_1(z) \rangle = -\frac{\frac{\pi}{2} U_m |\sin(\chi_d)|}{\Delta^2} \operatorname{atan}(k_u e) e \leq -\left[\frac{k_u \frac{\pi}{2} U_m |\sin(\chi_d)|}{\Delta^2} \right] e^2 \quad \forall z \in \mathcal{U}_1 = C_1 \tag{22}$$

According to [16, Theorem (3.2a)] there exists function $\rho_2 \in \mathcal{PD}$ such that:

$$\langle \nabla V(z), F_2(z) \rangle = -\rho_2(|z|) \quad \forall z \in \mathbb{R}^2 \tag{23}$$

Also for each $\eta = (q, z) \in D$, i.e $z \in D_q$ $\lambda \in \mathcal{K}_\infty$

$$\frac{V(g)}{V(z)} = \frac{1}{(H(z)+1)^2 + (H(z))^2} \leq 2 \tag{24}$$

where

$$H(z) = \frac{e}{\Delta(\tan(\psi_d - \chi_s) + \tan(\chi_s))} \quad \text{and} \quad (\min\{H(z)+1)^2 + (H(z))^2\} = 1/2$$

Thus, [14, (3.11)] holds for $\lambda(s) = 2s$. Due to the construction of D_1 and D_2 the variable z cannot reach the set D_1 from D_2 so solutions can not experience more than two jumps. Therefore Assumption 1 from [14, (Proposition 3.30)] holds with $J = 2$ and $\gamma \in \mathcal{K}$ arbitrary. □

VII. Simulation Results and Discussion

This section illustrates the docking maneuver and shows how the hybrid guidance strategy helps to achieve the maneuver objectives.

A. Configuration parameters

For the simulation we use the AUV model and parameters given in [17]. In order to achieve the desired states (ψ_d, U_{rd}) a feedback linearizing controller is used. The shape and dimensions of the docking station, that condition some of the parameters of the hybrid guidance controller, are based on the docking station described in [10].

The values that define the switching sets are $d_1 = 0.54[m]$, $d_2 = d_1/2$ and $\psi_{max} = 0.1[rad]$. The length of the *sliding path* is $l = 25[m]$. The AUV is initialized at position $p_0 = [-100, 0]$, facing straight to the entrance of the docking station $(\psi = \psi_{doc} = 0)$ with a velocity $(u = U_{doc} = 0.6[m/s])$.

B. Maneuver simulation

Figure 5 shows the result of the simulation of a complete docking maneuver. The current on this particular simulation was set to $V_x = -0.1[m/s]$, $V_y = -0.35[m/s]$. The arrows, representing the AUV are shaded according with the guidance law being used by the hybrid system, ILOS or SRG.

The vehicle begins at p_0 (see ①) controlled by the ILOS guidance which allows the vehicle to reach the *approaching path*. When the vehicle converges to the path ②, the yaw converges also to a ψ_{ss} that compensates for the effects of current, keeping a straight course. Once at ③ the AUV changes its objective and starts following the *sliding path*, using the hybrid guidance which keeps using ILOS at the beginning. When the vehicle fulfills the condition $(e, \psi_d \in D_2)$ described in Section VI, the vehicle is allowed to switch to the SRG ④. This controller combined with the presence of current, allows the vehicle to follow the sliding path while at the same time the yaw is forced to align with the docking station. Finally at the docking point ⑤ $(x = 0)$ the vehicle has successfully reached the docking station.

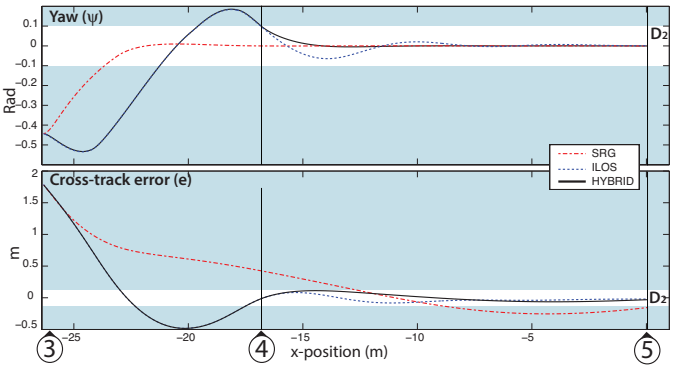

Fig. 6. Evolution of the yaw and the cross-track error and the yaw during the sliding path.

C. Sliding path

Figure 6 shows with more detail the evolution of the states when following the sliding path (between ③ and ⑤). The plot on top shows the yaw angle (ψ) with respect to the docking station centerline as the vehicle moves closer to it, while the second represents the cross-track error (e) to the *sliding path*. Note that ψ is perturbed by the vehicle dynamics and therefore ψ does not equal ψ_d during transients. The solid black line shows the evolution of the states for the simulation illustrated in Figure 5. The red and blue lines from Figure 6 show how the evolution of the states would be if only SRG (red) or only ILOS (blue) were used.

As it can be appreciated in Figure 6, the SRG allows the vehicle to align much faster with the docking station centerline, but this comes at the price of a slower convergence towards the path. The ILOS guidance instead adjusts the yaw

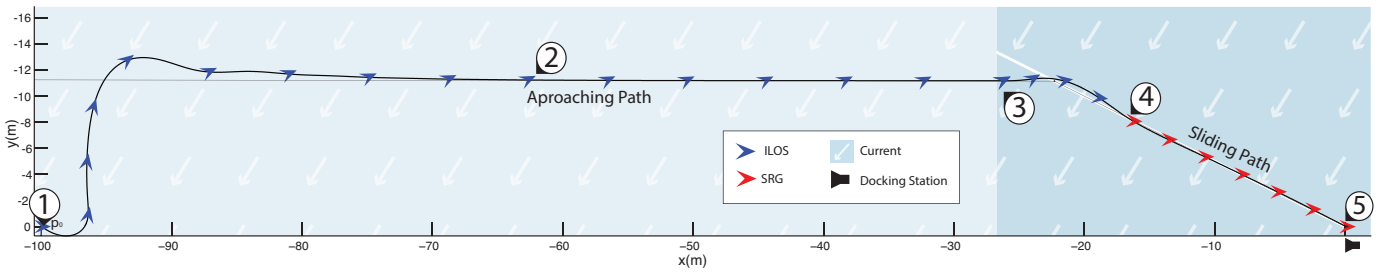

Fig. 5. Simulation of the docking maneuver

to control the approaching to the path, resulting in a much faster convergence to the path but more a more oscillating yaw angle. Once the hybrid system reaches region D_2 ④ it switches to SRG. Note that at this point the the black line corresponding to the hybrid system differs from the blue, because now the hybrid system is using SRG. This still allows the vehicle to converge to the path but also enforces the bearing to be zero. Comparing it with only ILOS (blue) it allows to converge faster to the desired yaw, and since the vehicle is already very close to the sliding path the slower convergence rate of the SRG has a small impact on the overall cross-track error, providing a less aggressive control that result in less oscillation.

D. Performance comparison

It is observed that in this particular case, the docking points ⑤ for the hybrid and the ILOS are very similar. In order to provide a better comparison, Figure 7 shows the docking points of 200 simulations for each controller and for two different current intensities. Mild currents are cross-currents $|V_y|$ ranging from 0 to $0.2m/s$ and strong currents range between $(0.2 - 0.4m/s)$. Both are uniformly and randomly distributed.

In Figure 7 a total of 1200 simulations are represented. Each dot represents the docking point ⑤ of each simulation and it is colored accordingly to the guidance used.

It results in a cloud of dots for each guidance illustrating the differences between them. A 1σ covariance ellipse is displayed to easily visualize the different guidances (Red=only SRG, blue=only ILOS and black=hybrid guidance).

In both current scenarios the SRG provides better angular accuracy, while ILOS provides a better position accuracy. Figure 7 also shows that stronger currents make the docking maneuver less accurate. In the mild currents scenario, it can be seen by that the hybrid guidance system provides a similar angular accuracy as the SRG, but much more precise in offset. However the hybrid system has a slightly bigger error in offset than only ILOS. In the strong current scenario the hybrid guidance performs better than the ILOS in both offset and angle. Also the hybrid guidance maintains a similar performance in offset error in both scenarios.

VIII. Conclusion

This paper has proposed a novel docking maneuver for underactuated AUVs consisting of a docking path and a combination of two path following guidance laws that enables the AUV to reach a docking station with a heading that is parallel to its entrance, in the presence of cross-currents. The paper proves the stability of the two guidance laws combined in a hybrid framework and the good behavior is further confirmed by simulations. Under the given parameters the simulations have also shown that the hybrid combination of the guidance law can provide better results than either guidance law alone, especially when currents are stronger. Future research will examine in detail the performance of the hybrid guidance when the AUV has imprecise estimates of the current.

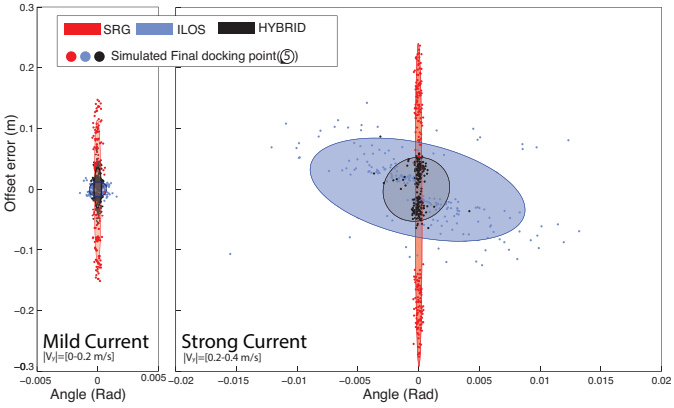

Fig. 7. Final docking point of 1200 simulations under different current conditions and guidance laws

Acknowledgments

This work was partly supported by the Research Council of Norway through the Centers of Excellence funding scheme, project No. 223254 AMOS, and project No. 205622.

References

[1] R. S. McEwen, B. W. Hobson, L. McBride, and J. G. Bellingham, "Docking control system for a 54-cm-diameter (21-in) auv," *IEEE Journal of Oceanic Engineering*, vol. 33, no. 4, pp. 550–562, Oct 2008.

[2] Hydroid, "Underwater mobile docking of autonomous underwater vehicles," in *IEEE, OCEANS*, Hampton Roads, VA, Oct 2012, pp. 1–15.

[3] M. D. Feezor, F. Y. Sorrell, P. R. Blankinship, and J. G. Bellingham, "Autonomous underwater vehicle homing/docking via electromagnetic guidance," *IEEE Journal of Oceanic Engineering*, vol. 26, no. 4, pp. 515–521, 2001.

[4] B. Allen, T. Austin, N. Forrester, R. Goldsborough, A. Kukulya, G. Packard, M. Purcell, and R. Stokey, "Autonomous docking demonstrations with enhanced REMUS technology," in *IEEE, OCEANS*, Boston, MA, 2006, pp. 1–6.

[5] A. Plueddemann, A. Kukulya, R. Stokey, and L. Freitag, "Autonomous underwater vehicle operations beneath coastal sea ice," *Transactions on Mechatronics*, vol. 17, no. 1, pp. 54–64, 2012.

[6] R. Stokey, B. Allen, T. Austin, R. Goldsborough, N. Forrester, M. Purcell, and C. von Alt, "Enabling technologies for REMUS docking: an integral component of an autonomous ocean-sampling network," *IEEE, Journal of Oceanic Engineering*, vol. 26, no. 4, pp. 487–497, 2001.

[7] H. Singh, J. G. Bellingham, F. Hover, S. Lemer, B. A. Moran, K. von der Heydt, and D. Yoerger, "Docking for an autonomous ocean sampling network," *IEEE, Journal of Oceanic Engineering*, vol. 26, no. 4, pp. 498–514, 2001.

[8] J.-Y. Park, B.-H. Jun, P.-M. Lee, Y.-K. Lim, and J.-H. Oh, "Docking problem and guidance laws considering drift for an underactuated auv," in *IEEE, OCEANS*. Santander, Spain: IEEE, 2011, pp. 1–7.

[9] K. Teo, E. An, and P. Beaujean, "A robust fuzzy autonomous underwater vehicle (auv) docking approach for unknown current disturbances," *Oceanic Engineering, IEEE Journal of*, vol. 37, no. 2, pp. 143–155, 2012.

[10] R. S. McEwen, B. W. Hobson, L. McBride, and J. G. Bellingham, "Docking control system for a 54-cm-diameter (21-in) AUV," *IEEE Journal of Oceanic Engineering*, vol. 33, no. 4, pp. 550–562, 2008.

[11] J.-Y. Park, B.-H. Jun, P.-M. Lee, J.-H. Oh, and Y.-K. Lim, "Underwater docking approach of an under-actuated auv in the presence of constant ocean current," *IFAC Proceedings Volumes*, vol. 43, no. 20, pp. 5–10, 2010.

[12] J.-Y. Park, B.-H. Jun, K. Kim, P.-M. Lee, J.-H. Oh, and Y.-K. Lim, "Improvement of vision guided underwater docking for small auv isimi," in *IEEE, OCEANS*. IEEE, 2009, pp. 1–5.

[13] W. Caharija, K. Y. Pettersen, M. Bibuli, P. Calado, E. Zereik, J. Braga, J. T. Gravdahl, A. J. Sørensen, M. Milovanović, and G. Bruzzone, "Integral line-of-sight guidance and control of underactuated marine vehicles: Theory, simulations, and experiments," *IEEE Transactions on Control Systems Technology*, vol. PP, no. 99, pp. 1–20, 2016.

[14] R. Goebel, R. G. Sanfelice, and A. R. Teel, *Hybrid Dynamical Systems: modeling, stability, and robustness*. Princeton University Press, 2012.

[15] P. Encarnaçao, A. Pascoal, and M. Arcak, "Path following for marine vehicles in the presence of unknown currents," in *Proceedings of SYROCO*, vol. 2, 2000, pp. 469–474.

[16] W. Caharija, "Integral line-of-sight guidance and control of underactuated marine vehicles," Ph.D. dissertation, Norwegian University of Science and Technology, 2014.

[17] T. Prestero, "Verification of a six-degree of freedom simulation model for the remus autonomous underwater vehicle," Ph.D. dissertation, Massachusetts Institute of Technology and Woods Hole Oceanographic Institution, 2001.